Isolation and Characterization of Endocardial Endothelial Cells from the Left Ventricular Wall and Outflow Tract of the Porcine Heart

Kathleen N. Brown[1], Hong Kim T. Phan[1], Elysa L. Jui[1], Marci K. Kang[1], Jennifer P. Connell[1], Sundeep G. Keswani[2], and K. Jane Grande-Allen[1]

[1]Department of Bioengineering, Rice University, Houston, TX

[2]Division of Pediatric Surgery, Department of Surgery, Texas Children's Hospital, Houston, TX

Abbreviated title: Isolation of Endocardial Endothelial Cells

Address for correspondence:

K. Jane Grande-Allen, Ph.D.

Department of Bioengineering

Rice University

6100 Main St., MS 142

Houston, TX 77005

Phone: 713-348-3704

Email: grande@rice.edu

Abstract

The heart contains six different types of endothelial cells, each with a unique function. We sought to characterize the endocardial endothelial cells (EECs), which line the chambers of the heart. EECs are relatively understudied, yet their dysregulation can lead to various cardiac pathologies. Due to the limited availability of this cell line, we developed a protocol for isolating EECs from porcine hearts and then compared their phenotype and fundamental behavior to a well-known comparator endothelial cell line, human umbilical vein endothelial cells (HUVECs). Compared with HUVECs, the EECs were slightly smaller, and stained positively for classic endothelial phenotypic markers such as CD31, von Willebrand Factor, and VE cadherin. The EECs proliferated more quickly than HUVECs, yet migrated more slowly to cover a scratch wound assay. Finally, the EECs maintained their robust endothelial phenotype (expression of CD31) through more than a dozen passages. In contrast, the HUVECs showed significantly reduced CD31 expression in later passages. These important phenotypic differences between EECs and HUVECs highlights the need for researchers to characterize specific cell lines when investigating their relevance to diseases of interest.

Introduction

Endothelial cells comprise 60% of the non-myocyte cellular composition of the heart (1). There are six endothelial phenotypes that can be found within the heart: valvular, endocardial, coronary arterial, venous, capillary, and lymphatic (2–4). Each endothelial phenotype within the cardiovascular system serves a unique function and therefore differs in structure and behavior (5). For example, valvular endothelial cells cover the surface of the aortic, mitral, pulmonary, and tricuspid valves within the heart and are exposed to a high volume of circulating blood and mechanical forces during the cardiac cycle, whereas cardiac lymphatic endothelial cells are dispersed throughout the myocardium to drain fluids from the tissue and sprout vessels in response to injury (1,3). It has even been demonstrated that valvular endothelial cells on opposing sides of the aortic valve have different phenotypic signatures that can be detected (6). Studies have shown that endothelial cells profoundly shift their behavior, morphology, and cellular signaling in response to pathological environments (4). Including region-specific endothelial cells in disease models can enhance understanding of the disease and increase understanding of disease mechanisms on the cellular level.

While the field of endothelial biology has expanded greatly in the past decade, there are many endothelial phenotypes that remain to be characterized. We sought to characterize the specific phenotype of endothelial cells that line the chambers of the heart, endocardial endothelial cells (EECs). To better understand the role of EECs in cardiac diseases, we created a protocol to isolate EECs and thereby study their unique phenotype. EECs are the innermost layer of the heart that serve as the barrier between circulating blood and the ventricular myocardium. This population of cells is exposed to

mechanical stimuli, including shear stresses due to cardiac blood flow. It has been shown that dysregulation of EECs leads to cardiac pathologies such as myocardial infarctions, atrial fibrillation, and thrombosis (7–9), yet these cells are relatively understudied compared to the coronary and aortic endothelium. Due to the limited availability of this cell line, we developed a protocol for isolating EECs from porcine hearts. We then investigated the unique phenotype and behavior of EECs in comparison to a well-known comparator endothelial cell line.

Materials and Methods

Preparation of reagents and workspace

In preparation for the heart dissection and enzymatic isolation of the EECs, the workspace and reagents were set up in advance. The following supplies were autoclaved: surgical tray, 600 mL beaker, two 1000 mL beakers, one pair of large surgical scissors, one pair of small curved surgical scissors, one pair of surgical hemostats, 12 cotton swabs, and two liters of phosphate buffered saline (PBS). Additionally, the following materials were gathered: spray bottle of 70% ethanol, six 8-ounce sterile specimen cups (VWR, #89125-846), 40 µm cell strainer (Corning, #352340), sterile towel drape (Fisher Scientific, #19-310-671). The dissociation solution was prepared using collagenase and dispase as the active enzymes. The stock collagenase solution was prepared by weighing out 25.2 mg of collagenase 2 (Worthington Biochemical, #LS004177) into a 50 mL tube. Next, 48.75 mL of Dulbecco's Modification of Eagle's Medium (Corning, #10-014-CV) and 1.25 mL of Penicillin-Streptomycin (Gibco, #15140122) were added to the tube, and the solution

was gently inverted to mix. The stock collagenase solution (final concentration of 0.05% collagenase) was then sterile filtered. The dissociation solution was prepared by adding 30 mL of the freshly prepared stock collagenase solution to a 50 mL tube, then adding 20 mL of dispase in Hank's balanced salt solution (Stemcell Technologies, #07913) to result in a 60% collagenase, 40% dispase solution, and gently inverting the tube to mix.

To prevent contamination, the heart dissection and isolation steps were performed in a biological safety cabinet (BSC), which required setting up the dissection workspace in advance. In an empty BSC, the three sterile beakers were brought into the hood. In the 600 mL beaker, 300 mL of 70% ethanol was added. The sterile surgical tools (scissors and clamp) were then brought into the hood and placed in the beaker with ethanol. Next, 800 mL of sterile PBS was added to both 1000 mL beakers. In one of the beakers, 40 mL of Antibiotic-Antimycotic (ABAM) (Gibco, #15240062) was added to create a 5% v/v solution. All the beakers containing the wash reagents remained at room temperature throughout the protocol. Finally, the sterile specimen cups, sterile drape, and sterile surgical tray were brought into the biological hood. The drape was opened and laid down first, then the surgical tray was placed on top of the drape. The lids of the specimen cups were removed so that the ventricles could easily be added to the cups.

Heart dissection

To obtain sufficient numbers of EECs, the isolation process requires fresh tissue from multiple porcine hearts. For each EEC harvest process, six porcine hearts were obtained from a local abattoir (Animal Technologies, Tyler, TX) and shipped overnight

on wet ice. Cells were collected from the hearts as soon as the package arrived to maintain cell viability. Fresh gloves were used to transport each heart from the packaging into the dissection workspace onto the surgical tray. The following procedure was completed for each heart individually while the other hearts remained on ice.

To obtain access to the left ventricle, the surrounding tissue was dissected off the heart, including the mitral valve. The large surgical scissors were used to remove the right and left atria from the heart to expose the ventricles of the heart. The right ventricular wall tissue was then dissected away, leaving the left ventricle intact. The aorta was also removed by cutting immediately below the aortic valve. An incision was made on the exterior of the left ventricle immediately below the epicardial fat band, being careful to cut through the ventricle wall for the entire circumference of the ventricle while leaving the mitral valve intact. Once this was complete, the mitral valve was attached to the ventricle only by the chordae tendineae. Using the small surgical scissors, each chordal attachment of the mitral valve was carefully dissected from their attachment at the papillary muscle within the left ventricle.

After this dissection step, the heart was placed into the 1000 mL beaker of PBS for a 5-minute rinse, then transferred using sterile hemostats to the 1000 mL beaker of PBS + ABAM for a second 5-minute rinse. After rinsing, the apex of the ventricle was placed into a sterile specimen cup, which was used to support the ventricle and hold it upright. If the ventricle was too thick to fit into the specimen cup, the exterior surface of the ventricle was trimmed down. The ventricle was then filled with PBS + ABAM, and set aside until all six hearts were similarly dissected and washed.

EEC Dissociation and Purification

After preparing the ventricles, the next step was to fill the ventricles with the dissociation solution. The PBS + ABAM solution was aspirated from each ventricle using a plastic aspirating tip (VWR, #414004-265), taking care to avoid puncturing the tissue. Next, each ventricle was filled with the dissociation solution. The volume of solution that each ventricle contained varied, but typically 7 mL of dissociation solution was needed per ventricle. The sterile cups were then sealed with their lids, transferred to a clean surgical tray, and incubated at 37°C for 90 minutes.

After the incubation step, the tray of ventricles was brought back into the BSC. The dissociation solution was removed from each ventricle and transferred to a 50 mL conical tube that was fitted with a 40 µm cell strainer to filter out tissue debris. The dissociation solution was pooled from all six hearts. The inner surface of each left ventricle was swabbed three times using two sterile cotton swabs per ventricle to remove any remaining endothelial cells. Each cotton swab was then held over the 50 mL collection tube and washed with 1 mL of the dissociation solution to remove the cells from the swab. This step was repeated for each ventricle.

Once all of the dissociation solution was collected, the tube was centrifuged for 5 minutes at 150 x*g* to obtain a cell pellet. The supernatant was aspirated, and the cell pellet was re-suspended in 10 mL of Endothelial Cell Growth Medium-2 (EGM-2, Lonza, #CC-3162). The cell suspension was plated into a 75 cm^2 tissue culture treated flask and cultured in a 5% CO_2 incubator at 37°C. The growth medium was changed every other day.

To purify the EECs from any other cells that may have been harvested during the dissociation process, the cells were sorted after they attained ~75% confluency. A magnetic bead sorting kit (CELLection Pan Mouse IgG Kit, Invitrogen, #11531D) was used according to manufacturer's instructions; the antibody used to coat the beads and sort the cells was PECAM-1 [CD31] Monoclonal Antibody (EMD Millipore, #MAB1393). Prior to characterization, the EECs were bead-sorted subsequently at passage 1 and passage 2 to ensure cell purity. Three populations of EECs were isolated and sorted before freezing and storing in liquid nitrogen until testing. The freezing media used to store the cells in was 80% EGM-2 media (Lonza, #CC-3162), 10% dimethyl sulfoxide (Sigma-Aldrich, #D2650), and 10% fetal bovine serum (FBS, Fisher Scientific, #FB12999102).

HUVECs Cell Culture

We sought to compare the phenotype of the primary EEC cell line to a standard endothelial cell line, human umbilical vein endothelial cells (HUVECs). The HUVECs were obtained commercially from Lonza (#C2519A). Once received, the HUVECs were seeded into a 75 cm^2 tissue culture treated flask with 10 mL of EGM-2 (Lonza, #CC-3162) and cultured in a 5% CO_2 incubator at 37°C. The growth medium was changed every other day. After expanding the HUVECs, the cells were frozen down and stored in liquid nitrogen until testing. The freezing media used to store the cells in was 80% EGM-2 media (Lonza, #CC-3162), 10% dimethyl sulfoxide (Sigma-Aldrich, #D2650), and 10% FBS (Fisher Scientific, #FB12999102).

Immunofluorescence staining of EECs

We stained the EECs for common endothelial markers to localize the proteins within the cells. To prepare cells for immunofluorescence staining, the EECs were seeded onto glass slides. Sterile glass slides were placed into 100 mm petri dishes and coated with a 5% w/v gelatin in PBS solution for 10 minutes. The gelatin solution was aspirated off the glass slide and the surrounding petri dish. EECs were seeded directly onto the gelatin coated glass slides at a density of 0.8 $x10^6$ cells per slide. The petri dish was then filled with 12 mL of EGM-2 media (Lonza, #CC-3162) and placed into an incubator at 37°C. The media on the petri dish was changed every other day until the cells reached confluency.

After culturing the EECs to confluence, the cells were stained for immunofluorescence imaging. The petri dish containing the glass slide with a confluent layer of EECs was removed from the incubator, and the media in the petri dish was aspirated off the cells. The glass slide of EECs was fixed with 4% paraformaldehyde at room temperature for 10 minutes. The samples were washed with PBS three times for 5 minutes each. To permeabilize the cells, 0.2% Triton X-100 was added to the samples for 15 minutes. The samples were again washed with PBS three times for 5 minutes each, then blocked with a solution of 1% w/v of bovine serum albumin (BSA) in PBS. After blocking, the samples were incubated with the primary antibody solutions overnight (suspended in 1% BSA in PBS, see **Table 1** for antibody ratios) at 4°C. The next day, the samples were washed with PBS three times for 5 minutes each, then incubated with the secondary antibody solutions (suspended in PBS, see **Table 1** for antibody ratios) at room temperature for 1 hour, while protected from light. The samples

were washed with PBS three times for 5 minutes each. Finally, two drops of ProLong Glass Antifade Mountant with NucBlue (Thermo Fisher, #P36981) were added to each glass slide of cells, and then a coverslip was added. The air bubbles that formed were pushed out of the mounting media utilizing a 200 µL pipette tip. The samples were cured at room temperature and protected from light for 12 hours before imaging. Samples were imaged on Nikon Ti2 eclipse and Nikon A1 confocal microscopes.

Scratch Wound Migration Assay

Endothelial cell migration rates are an important feature *in vivo*, as endothelial cells participate in wound healing processes throughout the vasculature (10). Therefore, we compared the migration rates of EECs and HUVECs *in vitro*. To prepare cells for a scratch wound migration assay, EECs and HUVECs were seeded into 6 well tissue culture treated plates at a density of 0.3 $x10^6$ per well. The cells were cultured with EGM-2 media (Lonza, #CC-3162) until confluency was reached. To begin the scratch wound assay, the media was aspirated from each sample, and the tip of a 1000 µL pipette tip was used to scratch a wound into the center of each well. Fresh media was added to each well, the well plate was taken immediately for imaging on a Nikon T2 eclipse microscope to obtain brightfield images of the 0 hour time point for each sample. The samples were then imaged at 4 hours, 8 hours, and 24 hours after the scratch was made. The images were analyzed in ImageJ using the wound healing size tool plugin created by Suarez-Arnedo (11), which detects the border of the wound created in each image and calculated the size of the wound or blank space on the sample. By

evaluating the size of the wound over time, this analysis allowed us to compare the migration rates of EECs and HUVECs.

Cell Proliferation Assay

When evaluating migration rates of the cells, we considered how proliferation of the cells could affect the result of the migration assay. Therefore, we evaluated the proliferation rates of HUVECs and EECs. To perform this assay, HUVECs and EECs were seeded into 96 well plates at a density of 5 $x10^3$ cells per well. The cells were cultured with EGM-2 media (Lonza, #CC-3162) and incubated for 0, 24, 48, 72, and 96 hours. At these specified time points, the media was removed from the wells and the cells were incubated in a solution containing 2 μM calcein AM in PBS (Live/Dead Assay, Thermo Fisher, #L3224) for 30 minutes and imaged immediately via immunofluorescence imaging on a Nikon T2 eclipse microscope. The images were processed in ImageJ and the particles were in the live channel were analyzed and quantified utilizing the software.

Flow Cytometry

Many cell types, especially primary cells, change phenotype after being cultured and passaged for long periods. we sought to assess how well EECs maintain their endothelial phenotype across passages, and to compare their performance to HUVECs by evaluating CD31 protein expression with flow cytometry. To prepare for flow cytometry, EECs and HUVECs were seeded into 75 cm^2 tissue culture treated flasks at a density of 2.1 $x10^6$ cells per flask. The cells were cultured with EGM-2 media (Lonza,

#CC-3162). When the cells reached ~75% confluency, the cells were then lifted and assessed by flow cytometry.

To lift the cells, the flask of cells was rinsed with PBS and then 10 mL of Accutase (Sigma-Aldrich, #A6964) was added to each 75 cm^2 flask of cells and incubated for 10 minutes at 37°C. After incubating the cells, the flasks were gently tapped to detach the cells from the flask. The Accutase solution was transferred to a conical tube and then centrifuged for 5 minutes at 150 x*g* to obtain a cell pellet. After centrifuging, the cells were resuspended in 1% FBS in PBS at a density of 1 $x10^6$ cells per 100 µL. At this point, the cells were divided into different microcentrifuge tubes for the testing conditions. The CD31 antibody conjugated to fluorescent molecule APC (Thermo Scientific, #MA5-16769, 10 µL) or the APC isotype control (Thermo Scientific, #17-4714-42, 5 µL) was added to their respective samples tubes at concentrations recommended by the manufacturer. The samples were protected from light and incubated with the antibody at room temperature for 15 minutes. After incubation, 1 mL of 1% FBS in PBS was added to each tube for washing. The samples were centrifuged to obtain a cell pellet, then the supernatant was removed using a micropipette tip. The samples were washed again by resuspending the cell pellet into 1 mL 1% FBS in PBS to each tube and centrifuged again to obtain a cell pellet. The supernatant was removed, and the cells were resuspended in ~500 µL 1% FBS in PBS and transfer to polystyrene 5 ml flow cytometry tubes (MTC Bio, #T9010). The samples were placed on ice and protected from light until flow cytometry could be performed. Flow cytometry was performed on a Sony MA900 flow cytometer, and analysis was performed in FlowJo Version 7.

Results

As demonstrated in brightfield images (**Figure 1**), the HUVECs cell line had a round and cobblestone morphology, which is characteristic to endothelial cells (4,10). The EECs had a round and cobblestone morphology, however there was elongation and swirling observed in the growth pattern as well. When comparing EECs to HUVECs, the cells were smaller and more elongated in their morphology.

Immunofluorescent staining was performed across the three populations of isolated EECs, and representative images are shown in **Figure 2**. In Row A, the EECs were stained for von Willebrand Factor (vWF), a protein that is only expressed in endothelial cells. vWF is contained within the Weibel-Palade bodies, which are storage granules that fuse in response to vessel injury to secrete vWF to initiate blood coagulation (12,13,9,4,14,15). vWF is located inside the cell membrane, and typically presents as small granules within the cells. This description is consistent with the staining shown in Row A, indicating the cells positively expressed von Willebrand Factor. In Row B, the EECs were stained for vascular endothelial cadherin (VE Cadherin), a protein that is expressed on the membrane or surface of endothelial cells (13,10,14,16–19). In Row B, the EECs positively expressed VE Cadherin at the cell-cell junctions. In Row C, the EECs positively expressed CD31 on the membrane of the cells. In Row D, the cells were stained with phalloidin, which selectively labels F-actin filaments that compose the cytoskeleton (10,12,16,20). The EECs positively stained for F-actin, and the stain demonstrates the distribution of actin filaments throughout the

cells. Thus, the EECs positively expressed essential endothelial markers: CD31, von Willebrand Factor, and VE-Cadherin, which confirms their endothelial phenotype.

The scratch wound assay, which was quantified by the ImageJ plugin, demonstrated that the migration of HUVECs and EECs progressed at different rates (**Figure 3**). The HUVECs migrated faster than the EECs to close the wound created at all time points evaluated (**Figure 4**). However, out of concern that proliferation might have influenced the results of this assay, we compared proliferation rates. As shown in **Figure 5**, we found that the HUVECs proliferated more slowly than did the EECs, with significantly fewer cells at the 48 and 96 hour timepoints. This result confirms that the migration rate assay performed evaluated migration accurately, and proliferation did not influence the outcome of the migration assay results. Therefore, we concluded that HUVECs migrated faster than EECs.

As shown in the flow cytometry data of **Figure 6**, the CD31 expression profile of the EECs and HUVECs shifted between Passage 4 and Passage 11. The three populations of EECs maintained high expression levels of CD31 between the passage numbers, however, it is also shown that the HUVECs expressed less CD31 at Passage 11 in comparison to Passage 4. This is further demonstrated in **Figure 7**, where the percentage of cells positively expressing CD31 at Passages 4 to 15 is graphed and compared between the three populations of EECs and the population of HUVECs. Each data point on the graph represents a passage number for that population, and is the amount of cells positively expressing CD31 within that passage number. When statistically compared, the percentage of positivity for CD31 across passage numbers was not statistically different between each of the three populations of EECs, however

the CD31 expression for HUVECs was significantly lower than each of the EECs populations. Thus, the EECs maintained their endothelial phenotype across high passage numbers, particularly when compared to HUVECs.

Discussion

Endocardial endothelial cells have been well characterized in development, as EECs form the inner layer of the heart tube during cardiac formation (21,22). EECs demonstrate their fascinating plasticity during cardiogenesis when they undergo endothelial-to-mesenchymal transition (EndMT) to contribute to heart valve formation (18,23). After development, EECs serve as the inner lining of the heart and regulate oxygen and nutrient supply, mediate immune cell trafficking, and secrete vital signaling molecules to surrounding tissues (9,20,22,24,25). As EECs play an essential role in cardiac formation and function, and dysfunction of EECs has been implicated in several cardiac diseases including congenital valve disease, hypoplastic left heart syndrome, and cardiac hypertrophy (22,26–28). There was initial speculation that EECs contribute to microvascular remodeling after myocardial infarctions, however this was disproven through genetic fate mapping, which demonstrated that mature EECs maintain their endocardial phenotype in this pathological environment (29,30).

Despite the importance of EECs in disease pathologies, this cell line is largely understudied in the context of adult cardiac endothelium in physiological and pathological disease states. This is an exciting opportunity for researchers to contribute to this body of work, but there are challenges in this effort. There are currently no EEC lines commercially available, and thus EECs must be isolated by the researcher from

fresh cardiac tissue. Therefore, a thorough protocol on how to isolate and sort these cells was greatly needed. By providing this protocol, the authors hope to empower other labs to incorporate EECs into their disease models for cardiac pathologies for congenital and adult cardiac disease states. The response of EECs to pathological environments has not been characterized, and could provide important insights into disease formation and future therapies. For modeling cardiac diseases related to the cardiac lining, it is important to include EECs in these models, as their response is considered to be more representative of *in vivo* behaviors (31). Recent studies have studied the unique proteomic signature of EECs, even in comparison to aortic endothelial cells (6,25).

HUVECs are often used as the endothelial model for diseases as they are easy to obtain, and have the morphological and phenotypical signatures that are common to endothelial cells. However, HUVECs are not viable in high passages, and deteriorate their endothelial integrity after passages 5-6 (10,13). Additionally, HUVECs are immune naïve in comparison to adult endothelial cells have developed immunological capabilities as they have been exposed to the native immune system before isolation (32). These factors highlight the pitfalls of using commercially available cell lines, and underscore the need for researchers to utilize endothelial cell lines that specific to the tissue region they are researching.

In this study, we demonstrated the morphological and functional characteristics of the EEC cell line. EECs demonstrate typical EEC phenotypic markers of endothelial cells, but are smaller and have a more elongated morphology than other common endothelial cell lines (4,10). We found that EECs maintained higher endothelial integrity

over high passages compared to HUVECs, a novel insight that could inform future researchers, when they are choosing a cell line, how many passages the cells will be used for.

EECs are not commercially available for any animal. Therefore, the researcher must isolate and purify the cell line themselves. Additionally, to obtain sufficient numbers of cells, the isolation described here involves isolating cells from 6 hearts to pool together for one cell line. This aspect remains challenging when trying to obtain EECs from human hearts, as they are a precious resource and cannot be obtained in such high quantities.

This study highlights the needs for researchers to characterize cell types that are specific to the disease they are studying. Too often, cell lines that are convenient to obtain are chosen to try to model diseases, but as shown here, there are important phenotypic differences for each cell type that could influence the findings of one's study. Through characterizing the EEC line, we demonstrated that EECs could be a great resource for researchers that desire to study cardiac cells over high passages, and model disease characteristics observed in left ventricular outflow tract pathologies.

In conclusion, we successfully isolated, purified, and cultured endocardial endothelial cells, the cells that line the left ventricle and left ventricular outflow tract of the heart. We demonstrated the robust endothelial phenotype of EECs, as the cells maintained their endothelial expression even to passage 15. We showed that there are important phenotypical differences between EECs and HUVECs, which emphasizes the need for researchers to characterize specific cell lines relevant to the diseases they are studying.

Acknowledgements

Financial support for this research was provided by a gift from Lew and Laura Moorman, NIH R01 HL140305 (to KJGA and SGK), NIH T32 HL007676 (for MKK), and NSF Graduate Research Fellowship Program (for KNB and ELJ).

References

1. Pinto AR, Ilinykh A, Ivey MJ, Kuwabara JT, D'Antoni ML, Debuque R, et al. Revisiting Cardiac Cellular Composition. Circ Res. 2016 Feb 5;118(3):400–9.
2. Ishii Y, Langberg J, Rosborough K, Mikawa T. Endothelial cell lineages of the heart. Cell Tissue Res. 2008 Aug 6;335(1):67.
3. Klaourakis K, Vieira JM, Riley PR. The evolving cardiac lymphatic vasculature in development, repair and regeneration. Nat Rev Cardiol. 2021 May;18(5):368–79.
4. Goncharov NV, Popova PI, Avdonin PP, Kudryavtsev IV, Serebryakova MK, Korf EA, et al. Markers of Endothelial Cells in Normal and Pathological Conditions. Biochem Moscow Suppl Ser A. 2020 Jul 1;14(3):167–83.
5. Aird WC. Endothelial Cell Heterogeneity. Cold Spring Harb Perspect Med. 2012 Jan;2(1):a006429.
6. Aneesh Kumar A, Ajith Kumar GS, Satheesh G, Surendran A, Chandran M, Kartha CC, et al. Proteomics Analysis Reveals Diverse Molecular Characteristics between Endocardial and Aortic-Valvular Endothelium. Genes (Basel). 2021 Jun 30;12(7):1005.

7. Smiljic S. The clinical significance of endocardial endothelial dysfunction. Medicina. 2017 Dec 1;53(5):295–302.
8. Kuruvilla L, Tr S, Kartha CC. Immortalization and Characterization of Porcine Ventricular Endocardial Endothelial Cells. Endothelium. 2007 Jan;14(1):35–43.
9. Schoner A, Tyrrell C, Wu M, Gelow JM, Hayes AA, Lindner JR, et al. Endocardial Endothelial Dysfunction Progressively Disrupts Initially Anti then Pro-Thrombotic Pathways in Heart Failure Mice. PLoS One. 2015 Nov 13;10(11):e0142940.
10. Medina-Leyte DJ, Domínguez-Pérez M, Mercado I, Villarreal-Molina MT, Jacobo-Albavera L. Use of Human Umbilical Vein Endothelial Cells (HUVEC) as a Model to Study Cardiovascular Disease: A Review. Applied Sciences. 2020 Jan;10(3):938.
11. Suarez-Arnedo A, Figueroa FT, Clavijo C, Arbeláez P, Cruz JC, Muñoz-Camargo C. An image J plugin for the high throughput image analysis of in vitro scratch wound healing assays. PLOS ONE. 2020 Jul 28;15(7):e0232565.
12. Brutsaert DL, De Keulenaer GW, Fransen P, Mohan P, Kaluza GL, Andries LJ, et al. The cardiac endothelium: Functional morphology, development, and physiology. Progress in Cardiovascular Diseases. 1996 Nov 1;39(3):239–62.
13. Bouïs D, Hospers GAP, Meijer C, Molema G, Mulder NH. Endothelium in vitro: A review of human vascular endothelial cell lines for blood vessel-related research. Angiogenesis. 2001 Jun 1;4(2):91–102.
14. Wautier JL, Wautier MP. Endothelial Cell Participation in Inflammatory Reaction. Int J Mol Sci. 2021 Jun 13;22(12):6341.

15. Kaufman DP, Sanvictores T, Costanza M. Weibel Palade Bodies. In: StatPearls [Internet]. Treasure Island (FL): StatPearls Publishing; 2021 [cited 2021 Sep 27]. Available from: http://www.ncbi.nlm.nih.gov/books/NBK535353/
16. Dejana E, Corada M, Lampugnani MG. Endothelial cell-to-cell junctions. The FASEB Journal. 1995;9(10):910–8.
17. Glaser DE, Gower RM, Lauer NE, Tam K, Blancas AA, Shih AJ, et al. Functional characterization of embryonic stem cell-derived endothelial cells. J Vasc Res. 2011;48(5):415–28.
18. Dye B, Lincoln J. The Endocardium and Heart Valves. Cold Spring Harb Perspect Biol. 2020 Dec 1;12(12):a036723.
19. Fan X, Cyganek L, Nitschke K, Uhlig S, Nuhn P, Bieback K, et al. Functional Characterization of Human Induced Pluripotent Stem Cell-Derived Endothelial Cells. Int J Mol Sci. 2022 Jul 31;23(15):8507.
20. Kuruvilla L, Kartha CC. Molecular mechanisms in endothelial regulation of cardiac function. Mol Cell Biochem. 2003 Nov;253(1–2):113–23.
21. Harris IS, Black BL. Development of the Endocardium. Pediatr Cardiol. 2010 Apr 1;31(3):391–9.
22. Feulner L, van Vliet PP, Puceat M, Andelfinger G. Endocardial Regulation of Cardiac Development. J Cardiovasc Dev Dis. 2022 Apr 19;9(5):122.
23. Nakano A, Nakano H, Smith KA, Palpant NJ. The developmental origins and lineage contributions of endocardial endothelium. Biochimica et Biophysica Acta (BBA) - Molecular Cell Research. 2016 Jul 1;1863(7, Part B):1937–47.

24. Ricard N, Bailly S, Guignabert C, Simons M. The quiescent endothelium: signalling pathways regulating organ-specific endothelial normalcy. Nat Rev Cardiol. 2021 Aug;18(8):565–80.
25. Jaleel A, Aneesh Kumar A, Ajith Kumar GS, Surendran A, Kartha CC. Label-free quantitative proteomics analysis reveals distinct molecular characteristics in endocardial endothelium. Mol Cell Biochem. 2019 Jan;451(1–2):1–10.
26. Klein A, Bayrau B, Miao Y, Gu M. Isolation of Endocardial and Coronary Endothelial Cells from the Ventricular Free Wall of the Rat Heart. JoVE (Journal of Visualized Experiments). 2020 Apr 15;(158):e61126.
27. Kuruvilla L, Nair RR, Umashankar PR, Lal AV, Kartha CC. Endocardial endothelial cells stimulate proliferation and collagen synthesis of cardiac fibroblasts. Cell Biochem Biophys. 2007;47(1):65–72.
28. Leask RL, Jain N, Butany J. Endothelium and valvular diseases of the heart. Microscopy Research and Technique. 2003;60(2):129–37.
29. Miquerol L, Thireau J, Bideaux P, Sturny R, Richard S, Kelly RG. Endothelial plasticity drives arterial remodeling within the endocardium after myocardial infarction. Circ Res. 2015 May 22;116(11):1765–71.
30. Tang J, Zhang H, He L, Huang X, Li Y, Pu W, et al. Genetic Fate Mapping Defines the Vascular Potential of Endocardial Cells in the Adult Heart. Circ Res. 2018 Mar 30;122(7):984–93.
31. Garbern JC, Mummery CL, Lee RT. Model Systems for Cardiovascular Regenerative Biology. Cold Spring Harb Perspect Med. 2013 Apr 1;3(4):a014019.

32. Tan PH, Chan C, Xue SA, Dong R, Ananthesayanan B, Manunta M, et al. Phenotypic and functional differences between human saphenous vein (HSVEC) and umbilical vein (HUVEC) endothelial cells. Atherosclerosis. 2004 Apr 1;173(2):171–83.

Table 1. Primary and secondary antibody ratios used for immunofluorescence staining.

Primary Antibody	Primary Antibody Ratio	Secondary Antibody	Secondary Antibody Ratio
Mouse PECAM-1 [CD31] (EMD Millipore, #MAB1393)	1:100	Goat anti-Mouse IgG, AlexaFluor 555 (Invitrogen, #A-21422)	1:100
Rabbit pAb to von Willebrand Factor (Abcam, #ab6994)	1:100	Goat anti-Rabbit IgG, AlexaFluor 532 (Thermo Fisher, #A-111009)	1:100
Rabbit pAb to VE Cadherin (Abcam, #ab33168)	1:500	Goat anti-Rabbit IgG, AlexaFluor 532 (Thermo Fisher, #A-111009)	1:100
Phalloidin conjugated to AlexaFluor 555 (Thermo Fisher, #A34055)	1:100		

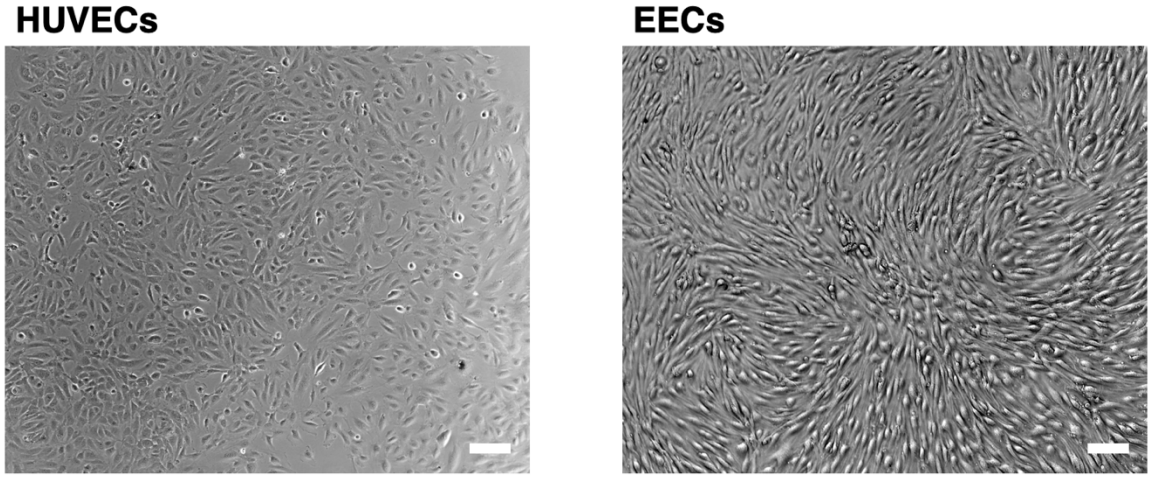

Figure 1. Brightfield images of human umbilical vein endothelial cells (HUVECs) and endocardial endothelial cells (EECs). Scale bar = 2000 μm.

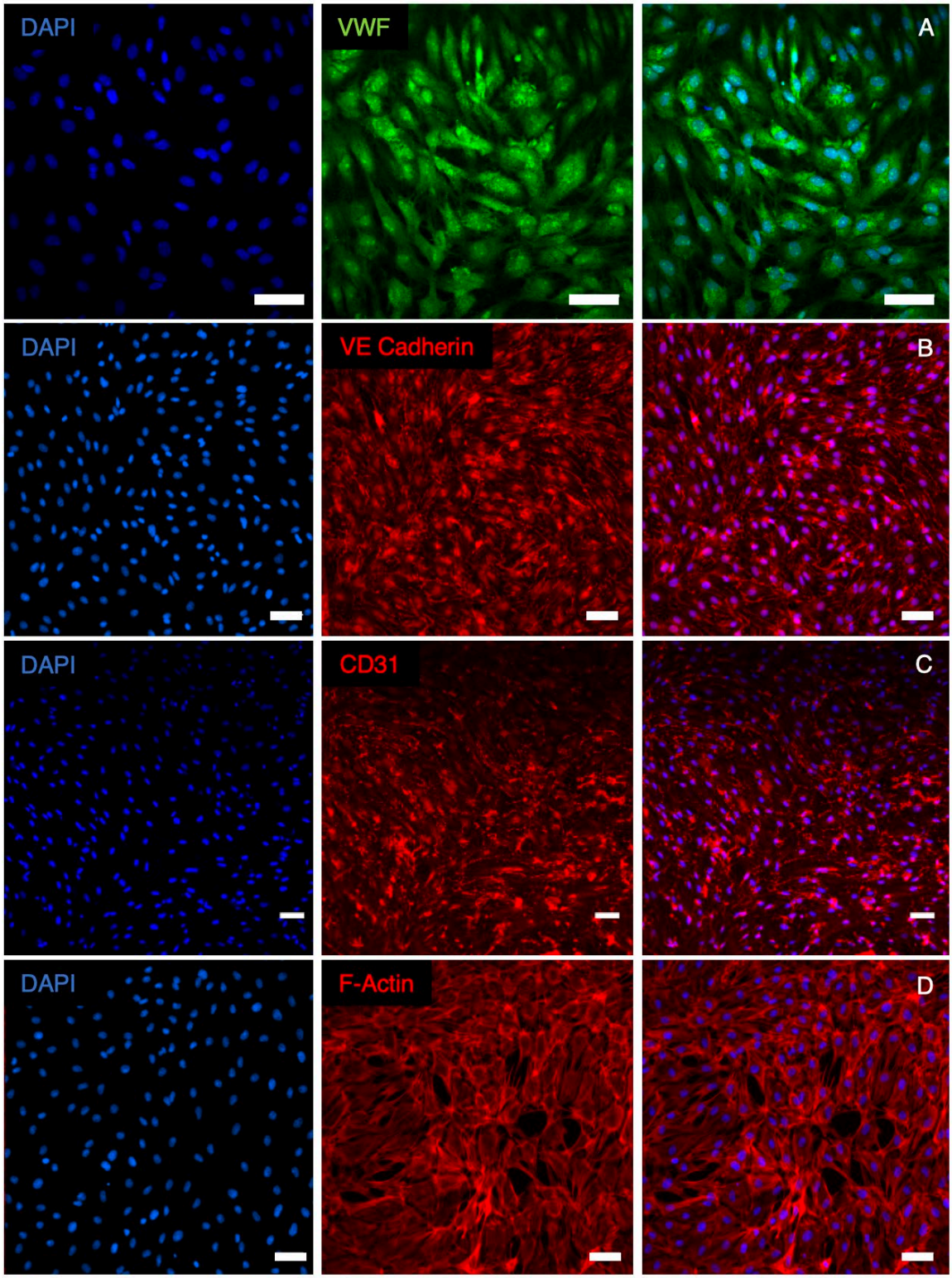

Figure 2. Immunofluorescence staining of EECs. In Row A, the EECs were stained for for von Willbrand Factor. In Row B, the EECs were stained for VE Cadherin. In Row C, the EECs were stained for CD31. In Row D, the EECs were stained for F-actin. Scale bar in Rows A, C, and D = 50 μm. Scale bar in Row B = 100 μm.

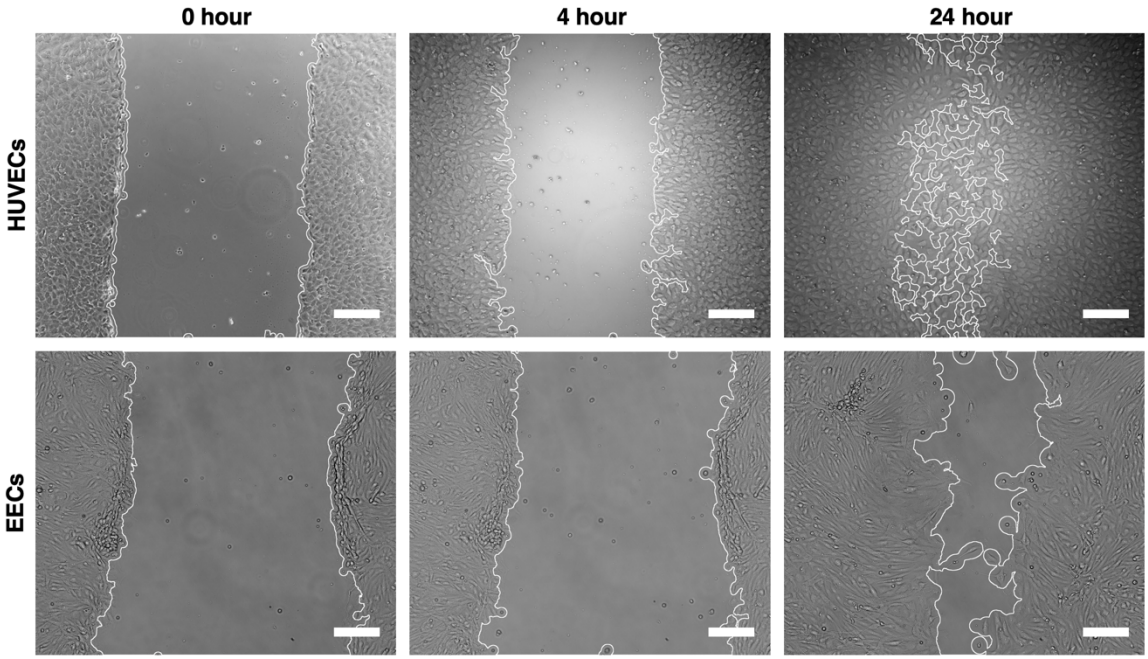

Figure 3. Brightfield images of HUVECs (top row) and EECs (bottom row) during the scratch wound migration assay at 0 hours, 4 hours, and 24 hours. The images shown also demonstrate the capability of the ImageJ wound healing size tool plugin, which oultined the edges of the wound created and calculated the size of the wound. Scale bar = 200 µm.

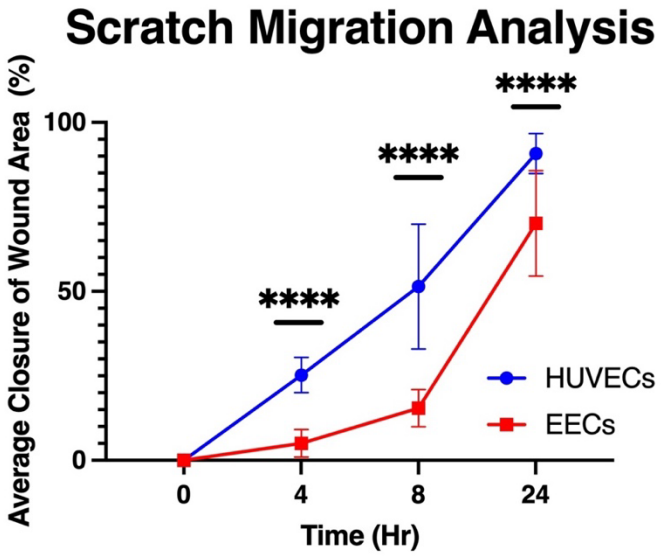

Figure 4. Graph comparing the migration rates of HUVECs and EECs at 0, 4, 8, and 24 hours. n=10. **** $p < 0.0001$.

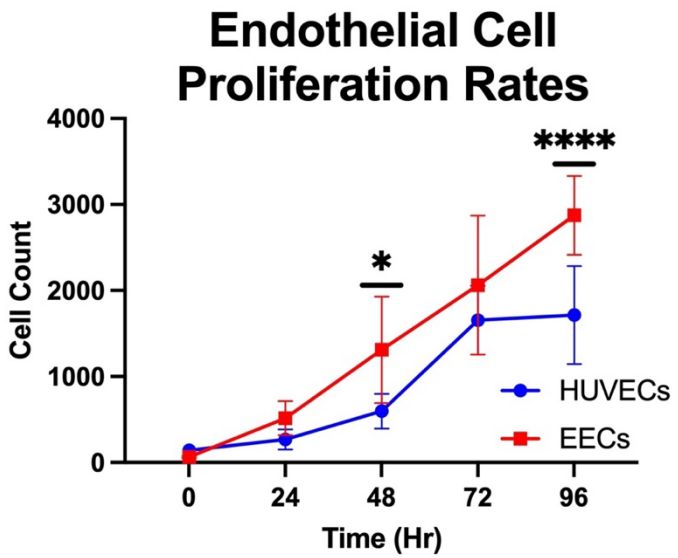

Figure 5. Graph comparing the proliferation rates of HUVECs and EECs calculated from live cell staining at 0, 24, 48, 72, and 96 hours. n=9. * p between 0.01-0.05; **** p < 0.0001.

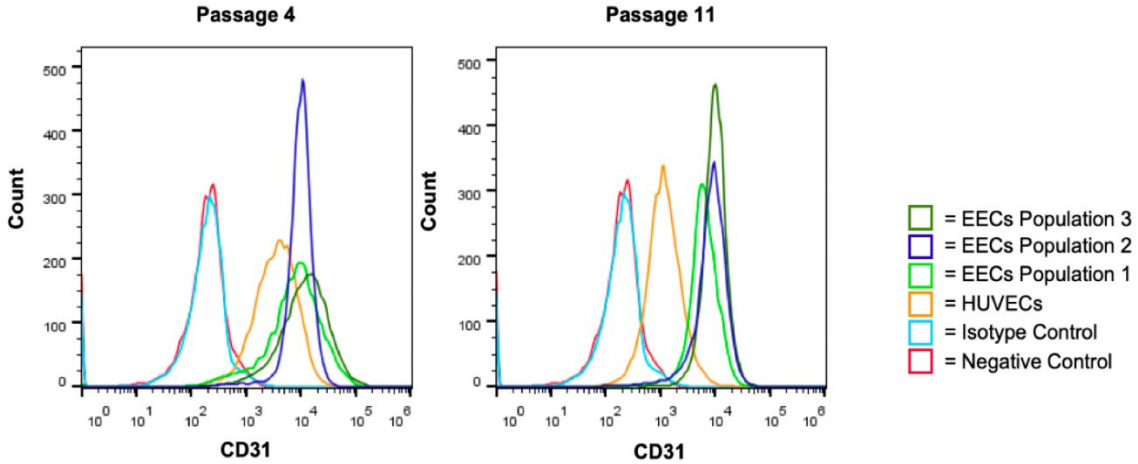

Figure 6. Flow cytometry results evaluating protein expression of CD31 betwen three populations of EECs, and a population of HUVECs across passages. Expression of CD31 across the samples can be seen at Passage 4 (graph on left) and Passage 11 (graph on right).

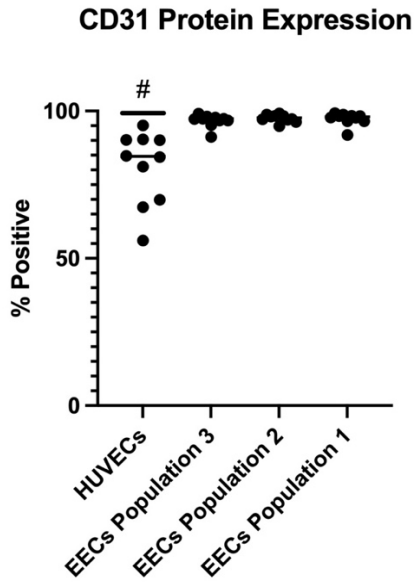

Figure 7. Graph of percentage of cells in each sample that positively expressed CD31 in the flow cytometry analysis between passage 4 - passage 15. Graph compares the HUVECs population to the three populations of EECs. # p between 0.0001-0.001 vs. all other groups.